Comparison of 2D and 3D Slope Stability Analysis Using Limit Equilibrium Method

Sumit Kumar[1], Brijbhan Rao[2], Shiva Shankar Choudhary[3], Avijit Burman[4] and
Lal Bahadur Roy[5]

Department of Civil Engineering, National Institute of Technology Patna, Patna-800005, India
[1]sumitk.phd19.ce@nitp.ac.in; [2]brijbhanr.phd19.ce@nitp.ac.in; [3]shiva@nitp.ac.in;
[4]avijit@nitp.ac.in; [5]lbroy@nitp.ac.in

Abstract. In slope engineering, two-dimensional (2D) limit equilibrium methods are most common. Two dimensional slope formulation has been done based on the assumption that plane strain conditions are applicable. However, if plane strain assumptions are invalidated, 3D slope analysis becomes unavoidable. It would be interesting to observe the difference between 2D and 3D slope analysis for any slope to study their mechanisms. In the present work, a homogenous soil slope is analyzed using both 2D and 3D formulation based on Bishop's Simplified Method (BSM). The digital elevation model (DEM) approach is used to build the slope's 3D geometry. The nature of failure surfaces, the distribution of normal force along the base of the failure surface, malpha (m_α) and the variation of base dip angles are plotted. The results indicate that 2D slope analysis usually yield conservative estimate of factor of safety (FS) than the 3D analysis. It is considered that 2D slope stability analysis always gives a more conserva- tive estimate of the three-dimensional (3D) slope stability problem

Keywords: Digital elevation model; Limit equilibrium method; Bishop Simplified analysis; Stability analysis; Factor of safety.

1   Introduction

The safety factor of the slope is essential from the engineering point of view, as a failure of the slope may cause several losses, such as economic losses, human losses, and obstacles in transportation. Natural and artificial slopes can be evaluated using several methods. These include finite difference, finite element, and limit equilibrium methods. Two-dimensional (2D) and three-dimensional (3D) approaches can assess slope stability. A slope must be appropriately analysed and designed to prevent such failures. The slope stability problem was initially formulated in two dimensions, as- suming plane strain conditions are valid. Hoek and Bra [1] stated that all slope stabil- ity analysis methodologies evaluate slopes in two dimensions, considering that the portion of the slope under study is a component of an infinitely long straight slope.2D analysis methods are still used because they are easy to make and take less time to run. For a very long time, the limit equilibrium method has been utilised for the pur- pose of analysing slope and earth dam stability issues [2]–[9]. Despite developments in numerical analytic methods like the finite element method, it remains significant in geotechnical engineering. The limit equilibrium method can offer an appropriate fac- tor of safety values if force and moment equilibrium are satisfied Duncan [4]. Accord- ing to Leshchinsky et al. [18], Ugai [19], and Leshchinsky and Baker [12], the factor of safety (FS) against slope failure in the limit equilibrium method (LEM) based slope stability formulation is the ratio of the forces preventing the failure mass from moving

downward to the forces attempting to cause instability. The limit analysis (LA) method-based slope stability formulation examines a slope that specifies the failure mechanism [20]–[22]. Clough & Woodward III [23] introduced FEM to geotechnical engineering. FEM is the best technique to address geotechnical problems since it can model nonlinear stress and strain. The SRT based on FEM may determine the 3D slope's *FS*. Despite taking longer than other methods, these are the most commonly employed to analyse 3D slope stability [24]–[28]. In this paper, both a 2D and a 3D formulation based on Bishop's Simplified Method are used to study a homogenous soil slope. This study developed a VBA-coded MS Excel spreadsheet platform incor- porating Bishop's simplified 2D slope stability analysis approach. A three-dimensional slope stability analysis was done using the Scoops 3D computer pro- gram. The Fortran source codes for Scoops-3D software that were available online were downloaded, compiled, and changed to meet our needs. The nature of failure surfaces, the distribution of normal force along the base of the failure surface, malpha (m_α) and the variation of base dip angles are compared for both 2D and 3D analysison a symmetric, homogenous slope. Generate 2D circular failure surface profiles using an entry-exit search strategy and then search for the critical failure surface (CFS) with a global minimum *FS*. A Digital Elevation Model (DEM) is used to make 3D slope geometry. The CFS and minimum FS are determined using a 3D box search technique that combines grid points with varied radius values to build spherical trial failure surfaces. It is helpful to illustrate the nature of the results obtained for two- dimensional and three-dimensional slope studies by comparing several associated parameters such as *FS*, interslice normal force, apparent dip angle, and m-alpha.

2   Methodology

In this paper, both a 2D and a 3D formulation based on Bishop's process of solving slope stability problems in two and three dimensions are comprised: i) making a 2D and 3D profile of slope geometry, ii) the limit equilibrium method based on Bishop's simplified method, is used to formulate the expression of the factor of safety (FS) against sliding; and iii) for 2D slope stability, VBA code-based spreadsheets are used to find the critical failure surface and the associated minimum FS. For 3D slope stability, a grid-based box search method is used by the Scoops 3D source code.

2.1   2D and 3D Slope Geometric Design

The geometry of the domain must be initially defined for both 2D and 3D slope assessments. In 2D slope stability analysis, a technique called the Entry, and Exit approach is employed. In Fig. 1, two thick (red) lines parallel the ground. These points will serve as the entry and exit points for the slip surfaces. The number of entries and exits can be determined by specifying the number of increments along these two lines. The 2D slip circle is made up of vertical slices, as shown in Fig. 2. Using the Digital Elevation Modelling (DEM) technique, the three-dimensional profile of a slope is created. A DEM input file content the surface elevation data of the DEM cell. The plan view of such DEM cell are shown in Fig. 3. The columns are extended vertically up to the bottom of the spherical failure surface from the slope's top surface.
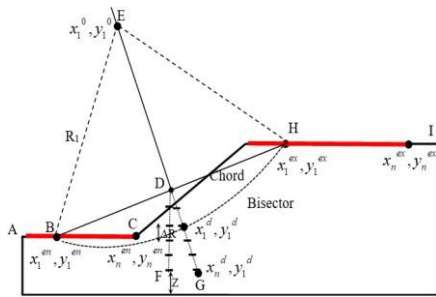
Fig. 1. Trial-slip entry and exit areas

Where,

$$\left(x_1^{en}, y_1^{en} \quad x_2^{en}, y_2^{en} \quad \ldots \quad x_n^{en}, y_n^{en} \right)^T \quad \text{is entry points;}$$

$$\left(x_1^{ex}, y_1^{ex} \quad x_2^{ex}, y_2^{ex} \quad \cdots \cdots \quad x_n^{ex}, y_n^{ex} \right)^T \text{is exit points;}$$
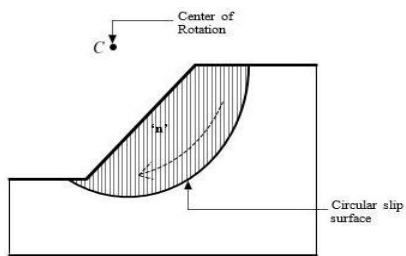
Fig. 2. 2D slope profile with vertical slice
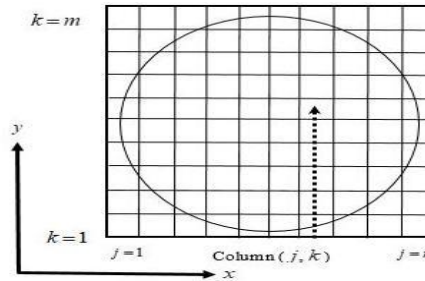
Fig. 3. Potential sliding mass divided in vertical columns

2.2   2D formulation of Bishop Simplified Analysis

Figure 4 represent the free body diagram of ith slice subjected to all possible combination of forces.
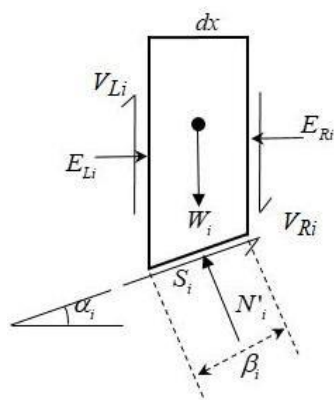
Where, $W_i \rightarrow$ Weight of ith slice; N_i'= Effective normal force at the bottom of ith slice; $N_i' = N_i - u_i\beta_i$; N_i= Normal force at i^{th} slice; u_i= Pore pressure at i^{th} slice; S_i= Mobilized shear force at the bottom of ith slice; E_{Li}, E_{Ri} Left and right interslice normal forces acting on i^{th} slice; V_{Li}, V_{Ri} Left-and-right interslice shear forces on i^{th} slice; dx Each width slice; β_i = Base Length of ith slice

Fig. 4. Free body diagram of ith slice

As mentioned earlier, Bishop simplified analysis satisfies the moment equilibrium condition for sliding mass $\sum\limits_{i=1}^{nslice} M_{ci} = 0$ about its center of rotation (C) for calculating *FS*, which is given in Eq.1.

$$\sum_{i=1}^{nslice} W_i x_i - \sum_{i=1}^{nslice} S_i r_i - \sum_{i=1}^{nslice} N_i f_i = 0 \tag{1}$$

Forces exerted on each slice are determined by limit equilibrium. The summation of forces on each slice determines mass equilibrium. In BSM, it is required to compute the force equilibrium in the vertical direction on the base of each slice to get the nor- mal force. In equation form, in the absence of pore water pressure, the base normal is defined as:

$$N'_i = \frac{V_{Ri} - V_{Li} + W_i - \dfrac{c'_i \, \beta_i \, \sin\alpha_i}{FS}}{\cos\alpha_i + \dfrac{\tan\phi'_i \, \sin\alpha_i}{FS}} \tag{2}$$

Where, $\cos\alpha_i + \dfrac{\tan\phi'_i \, \sin\alpha_i}{FS} = $ m-alpha (m_α) $\tag{3}$

Mobilized shear force at the base of each slice (S_i) can be represented as shown as:

$$(S_i) = \frac{c'_i \, \beta_i + N'_i \, \tan\varphi'}{FS} \tag{4}$$

In the absence of pore-water pressure, the Bishop's Simplified factor of safety equation can be expressed as:

$$\text{Factor of Safety } (FS) = \frac{\sum\limits_{i=1}^{n\,slices} \left[\left(c'_i \beta_i + \left(N_i - u_i \beta_i \right) \tan\phi'_i \right) r_i \right]}{\sum\limits_{i=1}^{n\,slices} \left[W_i x_i - N_i f_i \right]} \tag{5}$$

2.3   3D formulation of Bishop Simplified Analysis

Figure 5 represents the free body diagram of the *j,k* column as no external force was acting on the column subjected to all possible combinations of forces.

Where,
W is weight of column; $E_{x_{j,k}}$, $E_{y_{j,k}}$ = x and y directions inter-column normal force; $H_{x_{j,k}}$, $H_{y_{j,k}}$ = Horizontal shear force in y-z plane; ;$X_{x_{j,k}}$, $X_{y_{j,k}}$ = Inter-column shearforce in x-z plane; ; $N_{j,k}$, $U_{j,k}$ = effective normal force and base pore water force; $S_{j,k}$ = Mobilized shear force acting on base; $\alpha_{j,k}$ = Slide angle relative to the x–y plane; α_x, α_y = Base inclination in x-z and y-z planes at the middle of each column.

Fig. 5. Free body diagram of *j,k* column

The Scoops3D application employs the 3D extension of Bishop's 2D formulation Reid et al. [29] under the methodology proposed by previous researchers [14], [30].

The vertical normal force component is resolved using the vertical force equilibrium equation for a single column [14], [30] in terms of trial surface dip angle at column base. Bishop's approach states that the global resisting moment must equal the driving moment in order to keep moment equilibrium. The global moment equilibrium for all columns can be calculated as shown in Eq. (6).

$$\sum M = \sum R_{j,k} \frac{c_{j,k} A_{j,k} + (N_{j,k} - u_{j,k} A_{j,k}) \tan\phi_{j,k}}{F} - \sum W_{j,k} R_{j,k} m_z \tag{6}$$

The normal force is found using the vertical force of the equation as shown in Eq. (7).

$$N_{j,k} = \frac{W_{j,k} - c'_d A_{j,k} m_z + u_{j,k} A_{j,k} \tan\phi'_d m_z}{(\cos\varepsilon_{j,k} + \tan\phi'_d m_z)} \tag{7}$$

Here, $\cos\varepsilon_{j,k} + \tan\phi'_d m_z = m_{\alpha_{j,k}}$; $c'_d = \dfrac{c_{k,l}}{F}$; $\tan\phi'_d = \dfrac{\tan\phi_{k,l}}{F}$ and $m_z = \sin\alpha_{k,l}$

After simplifying and noting that the column base's a horizontal area, $A_{h_{k,l}} = A_{k,l}\cos\varepsilon_{k,l}$, FS is now represented by Eq. (8):

$$FS = \frac{\sum R_{j,k}\left(c_{j,k}A_{h_{j,k}} + \left(W_{j,k} - u_{j,k}A_{h_{j,k}}\right)\tan\phi_{j,k}\right)/m_{\alpha_{j,k}}}{\sum W_{j,k}R_{j,k}m_z} \tag{8}$$

Here, $c_{j,k}$ = the effective cohesion ; $\emptyset_{j,k}$ = the effective internal friction angle; $R_{j,k}$ is the distance from the j,k column's trial slip region to its axis of rotation, $N_{j,k}$ is the normal force on j,k column, $u_{j,k}$ is pore water pressure, $A_{j,k}$ is the trial surface area of column, $W_{j,k}$ is the weight of the column; $C_{j,k}$ is the angle between the inclined surface at the bottom of the slice and the horizontal x axis. $\alpha_{j,k}$ is apparent dip angle held between azimuthal direction and the direction of slip. This angle i.e. $\alpha_{j,k}$ for any col- umn j,k can be calculated using Eq. (9).

$$\alpha_{j,k} = \tan^{-1}\left[\left(\partial z/\partial x\right)\cos\delta + \left(\partial z/\partial y\right)\sin\delta\right] \tag{9}$$

3   Results and Discussion

In this work, the two- and three-dimensional slope stability analyses for determining the critical failure surface and the associated minimum FS are carried out. The Bishop simplified analysis was used to determine the CFS and FS of the 2D and 3D slopes. A homogeneous soil slope by Donald and Giam [31] was chosen for an analysis whose height is 10.0 m and a gradient of 1V:2H (where V stands for vertical and H stands for horizontal). The material properties of the slope are: cohesion (c') = 3.0 kN/m^2, angle of internal friction (ϕ') = 19.60^0 and unit weight (Υ) =20.0 kN/m^3. The nature of failure surfaces, the distribution of normal force along the base of the failure surface, malpha (m_α) and the variation of base dip angles are plotted for 2D and 3D, respectively. The performance of the two-dimensional slope is examined using the Visual Basic for Applications (VBA) program integrated into the Excel software. An Excel VBA program produced the two-dimensional failure slope in Fig. 6, along with the material input parameters.
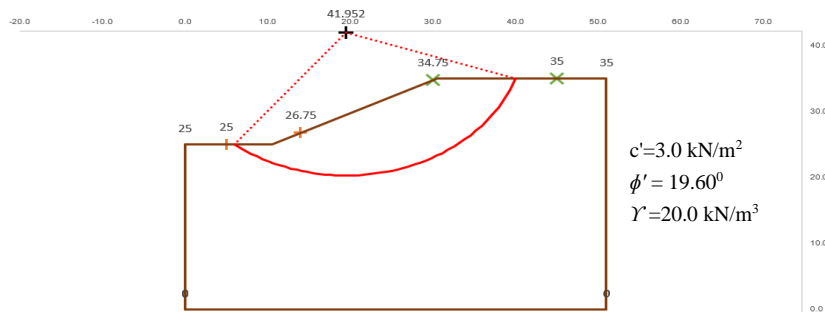
Fig. 6. Results evaluated of 2D slope stability from VBA code-based program

A digital elevation model (DEM) input file is required to produce the 3D geometric slope profile. In this work, the dimensions of the 3D slope profile in lateral and longi-

tudinal directions are considered to be 51 m. The current DEM grid has 102 and 101division on x and y-axes. With 0.5 m per column DEM cell resolution, the slope has 10302 columns. This paper examines a symmetric geometry and loading slope problem. A slope's CFS should be on its neutral plane, as shown in Fig. 7.
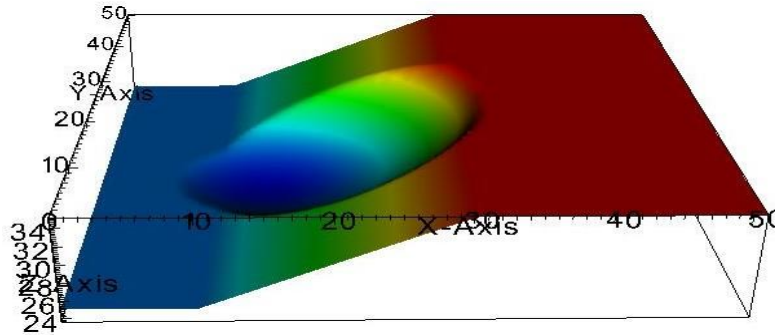
Fig. 7. 3D View of critical slip surface

The 2D and 3D FS values for the homogenous soil are reported in Table 1. Table 1 demonstrates that the FS results reported by earlier researchers, Reid et al. [29] are in extremely good agreement with one another. When examined in the 2D slope stability analysis in the current work for homogeneous soil, FS values have decreased as expected.

Table 1. FS results of 2D and 3D slope stability analysis.

Scenario	Present work (2D Slope stability)	Present work (3D slope stability)	Reid et al. (2015) CLARA-W (2D slope stability)	Reid et al. (2015) CLARA-W (3D slope stability)
Cell Size	0.5	0.5	0.5	-
Case 1 ($r_u = 0$)	0.986	1.03	0.99	1.04

3.1 Comparative study of homogeneous soil for 2D and 3D Slope Stability Analysis

At the base of the 2D and 3D columns for homogeneous soil, the responses to normal forces, apparent dip angles, and m-alpha were compared in order to assess the relative variation of the results. All of these findings came about as a result of a mid-plane-based Coarse to fine search. Fig. 8 depicts the fluctuation of normal forces operating at the base slices of columns along the slope's lateral direction. As can be shown from Fig. 8, for homogenous soils, normal force is depicted in the direction of failure mass sliding (i.e. lateral) for any continuous collection of slices and columns. The value of normal forces in 2D slope stability analysis was evaluated higher than in 3D.
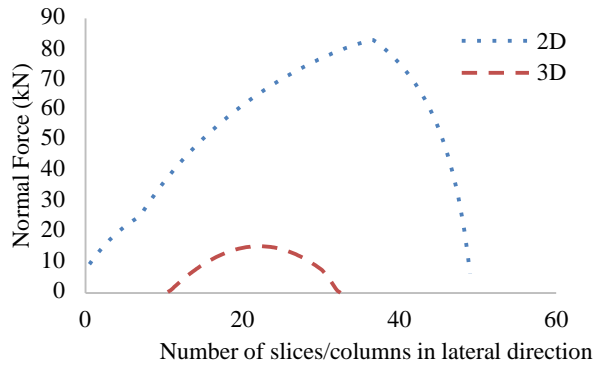
Fig. 8. Normal forces vs. Number of slices/columns in lateral direction

Fig. 9 reveals that there is a reduction in apparent dip angles in 2D slope stability analysis. Fig. 9 shows the distribution of apparent dip angles along the lateral direction. A spherical surface specifies the slip base in 3D slope analysis. As a result, some of the columns close to the sliding surface's toe may dip in the opposite direction from the slide direction. This results in a negative dip in the apparent dip angle near the slide's toe about the slide direction, as shown in Fig. 9.
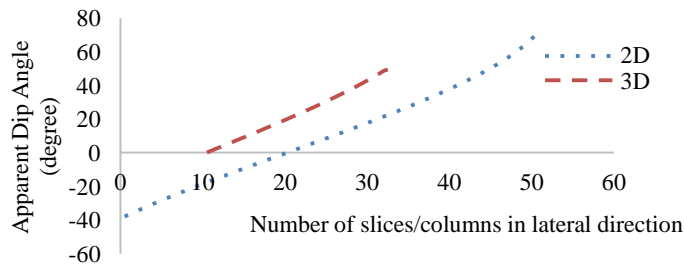
Fig. 9. Apparent dip angles vs. Number of slices/columns in lateral direction

Fig. 10 presents the results of m-alpha vs. apparent dip angles, which reduce the m-alpha value in the 2D slope stability analysis compared to the 3D slope stability analysis. The plot of m-alpha vs. apparent dip angles represents the smooth curve for homogeneous soils in both 2D and 3D slope stability analysis.
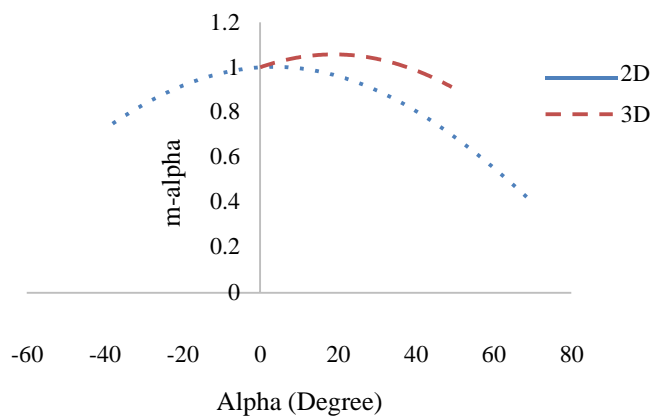
Fig. 10. m-alpha vs. apparent dip angle in lateral direction

4   Conclusions

The Visual Basic for Applications (VBA) code-based program and the Scoops 3D modified computer program are used for two-dimensional, and three-dimensional slope stability structures, respectively, and are compared in this work. Bishop's (1955) approach, a limit equilibrium methodology, determines slice failure for a 2D slope and spherical failure for a 3D slope. A VBA code-based program can be used to define the geometry of a 2D slope, and a digital elevation modelling (DEM) techniquecan be used to describe the geometry of a 3D slope. A DEM file is created using MS- Excel. In 3D slope stability investigations, a coarse-to-fine (CF) search is performed to find the CFS and minimum FS. It is shown that the given significantly affects the value of normal force, apparent dip angle, and m-alpha by calculations carried out in 2D and 3D using the VBA code and scoops3D program. The normal force values from the 2D slope are higher than those from the 3D slope, but the apparent dip an- gles and m-alpha are less, according to plots of normal forces, apparent dip angles, and m-alpha along lateral slope directions. In homogeneous soils, the 3D slope meas- ure gives higher FS values than the 2D slope measure.

References

1. E. Hoek and J. D. Bray, *Rock slope engineering*. CRC Press, 1981.
2. W. Fellenius, "Calculation of stability of earth dam. In Transactions. 2nd Congress Large Dams," vol. 4, pp. 445–462, 1936.
3. A. W. Bishop, "THE USE OF THE SLIP CIRCLE IN THE STABILITY ANALYSIS OF SLOPES," *First Tech. Sess. Gen. Theory Stab. Slopes*, 1955.
4. J. M. Duncan, "State of the art: limit equilibrium and finite-element analysis of slopes," *J. Geotech. Eng.*, vol. 122, no. 7, pp. 577–596, 1996.
5. N. R. Mongenstern and V. E. Price, "The Analysis of stability of general slide surfaces," *Geotechnique*, vol. 15, pp. 79–93, 1965.
6. E. Spencer, "A method of analysis of the stability of embankments assuming parallel inter-slice forces," *Geotechnique*, vol. 17, no. 1, pp. 11–26, 1967.

7. E. Spencer, "Thrust line criterion in embankment stability analysis," *Geotechnique*, vol. 23, no. 1, pp. 85–100, 1973.

8. N. Janbu, "Application of composite slip surface for stability analysis," in *Proceedings of European Conference on Stability of Earth Slopes, Sweden, 1954*, 1954, vol. 3, pp. 43–49.

9. Z.-Y. Chen and N. R. Morgenstern, "Extensions to the generalized method of slices for stability analysis," *Can. Geotech. J.*, vol. 20, no. 1, pp. 104–119, 1983.

10. H. J. Hovland, "Three-dimensional slope stability analysis method," *J. Geotech. Eng. Div.*, vol. 103, no. 9, pp. 971–986, 1977.

11. R. H. Chen and J. Chameaut, "Three-dimensional limit equilibrium analysis of slopes," no. 1, 1983.

12. D. Leshchinsky and R. Baker, "Three-dimensional slope stability: end effects," *SoilsFound.*, vol. 26, no. 4, pp. 98–110, 1986.

13. Z. Xing, "Three-dimensional stability analysis of concave slopes in plan view," *J. Geotech. Eng.*, vol. 114, no. 6, pp. 658–671, 1988.

14. O. Hungr, "An extension of Bishop's simplified method of slope stability analysis to three dimensions," *Geotechnique*, vol. 37, no. 1, pp. 113–117, 1987.

15. L. Lam and D. G. Fredlund, "A general limit equilibrium model for three-dimensional slope stability analysis," *Can. Geotech. J.*, vol. 30, no. 6, pp. 905–919, 1993.

16. Z. Chen, X. Wang, C. Haberfield, J. H. Yin, and Y. Wang, "A three-dimensional slope stability analysis method using the upper bound theorem Part I: Theory and methods," *Int. J. Rock Mech. Min. Sci.*, vol. 38, no. 3, pp. 369–378, 2001, doi: 10.1016/S1365-1609(01)00012-0.

17. Y. M. Cheng and C. J. Yip, "Three-Dimensional Asymmetrical Slope Stability Analysis Extension of Bishop ' s , Janbu ' s , and Morgenstern – Price ' s Techniques," vol. 133, no. December, pp. 1544–1555, 2007.

18. D. Leshchinsky, R. Baker, and M. L. Silver, "Three dimensional analysis of slope stability," *Int. J. Numer. Anal. Methods Geomech.*, vol. 9, no. 3, pp. 199–223, 1985.

19. K. Ugai, "Three-dimensional stability analysis of vertical cohesive slopes," *Soils Found.*, vol. 25, no. 3, pp. 41–48, 1985.

20. D. C. Drucker, H. J. Greenberg, and W. Prager, "The safety factor of an elastic-plastic body in plane strain," 1951.

21. D. C. Drucker and W. Prager, "Soil mechanics and plastic analysis or limit design," *Q. Appl. Math.*, vol. 10, no. 2, pp. 157–165, 1952.

22. Y. M. Cheng, "Location of critical failure surface and some further studies on slope stability analysis," *Comput. Geotech.*, vol. 30, no. 3, pp. 255–267, 2003.

23. R. W. Clough and R. J. Woodward III, "Analysis of embankment stresses and deformations," *J. Soil Mech. Found. Div.*, vol. 93, no. 4, pp. 529–549, 1967.

24. B. Jeremić, "Finite element methods for 3D slope stability analysis," *Proc. Sess. Geo-Denver 2000 - Slope Stab. 2000, GSP 101*, vol. 289, pp. 224–238, 2000, doi: 10.1061/40512(289)17.

25. K. Ugai and D. O. V Leshchinsky, "Three-dimensional limit equilibrium and finite element analyses: a comparison of results," *Soils Found.*, vol. 35, no. 4, pp. 1–7, 1995.

26. D. V. Griffiths and R. M. Marquez, "Three-dimensional slope stability analysis by elasto-plastic finite elements," *Geotechnique*, vol. 57, no. 6, pp. 537–546, 2007, doi: 10.1680/geot.2007.57.6.537.

27. D. Tan and S. K. Sarma, "Finite element verification of an enhanced limit equilibrium method for slope analysis," *Géotechnique*, vol. 58, no. 6, pp. 481–487, 2008, doi: 10.1680/geot.2007.00084.

28. M. K. Kelesoglu, "The evaluation of three-dimensional effects on slope stability by the strength reduction method," *KSCE J. Civ. Eng.*, vol. 20, no. 1, pp. 229–242, 2016, doi: 10.1007/s12205-015-0686-4.

29. M. E. Reid, S. B. Christian, D. L. Brien, and S. Henderson, "Scoops3D—software to analyze three-dimensional slope stability throughout a digital landscape," *US Geol. Surv. Tech. Methods, B.*, vol. 14, 2015.

30. O. Hungr, F. M. Salgado, and P. M. Byrne, "Evaluation of a three-dimensional method of slope stability analysis," *Can. Geotech. J.*, vol. 26, no. 4, pp. 679–686, 1989, doi: 10.1139/t89-079.

31. I. B. Donald and P. S. K. Giam, "The ACADS slope stability programs review," in *International Symposium on Landslides*, 1995, pp. 1665–1670.